Inorganic Chemistry

Article

pubs.acs.org/IC

Cd(II)-MOF: Adsorption, Separation, and Guest-Dependent Luminescence for Monohalobenzenes

Lei Wang,[†,‡] Yan-An Li,[†] Fan Yang,[†] Qi-Kui Liu,[†] Jian-Ping Ma,[†] and Yu-Bin Dong*[,†]

[†]College of Chemistry, Chemical Engineering and Materials Science, Collaborative Innovation Center of Functionalized Probes for Chemical Imaging, Key Laboratory of Molecular and Nano Probes, Ministry of Education, Shandong Normal University, Jinan 250014, People's Republic of China

[‡]Department of Pharmacy, Binzhou Medical University, Yantai 264003, People's Republic of China

Supporting Information

ABSTRACT: A series of isostructural 2-fold interpenetrating 2D Cd(II)-MOFs, namely G⊂$CdL_2(OTs)_2$ (G = THF (**1**), PhF (**2**), PhCl (**3**), PhBr (**4**), PhI (**5**), L = 1,2-bis[(3-(pyridin-4-yl)phenoxy]ethane, and OTs^- = *p*-toluenesulfonate anion), have been successfully synthesized from the flexible ethylene glycol ether-bridging ligand **L** and $Cd(OTs)_2$ in solution. The $CdL_2(OTs)_2$ framework contains squarelike nonpolar channels, and the encapsulated guest molecules can be removed by heating (150 °C) to generate a guest-free host framework which is able to reversibly adsorb monohalobenzenes PhX (X = F, Cl, Br, I) in the liquid phase under ambient conditions without loss of framework integrity. Furthermore, it can effectively separate these monohalobenzenes and exhibits a clear affinity for monohalobenzenes according to the following order: PhI > PhBr > PhCl > PhF. In addition, PhX⊂$CdL_2(OTs)_2$ exhibits guest-dependent luminescence properties.

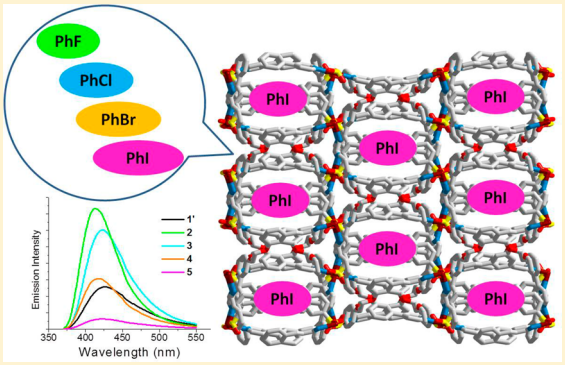

INTRODUCTION

Metal−organic frameworks (MOFs), as an emerging class of porous inorganic−organic hybrid materials, have attracted considerable interest in materials science due to their diverse potential applications. One of the most promising applications for MOFs might be their use as porous materials for adsorption and separation.[1] In principle, the specific pore size and inner microenvironment in MOFs could be realized by judicious choice of the organic ligands and inorganic metal nodes. Such MOFs might offer a possibility to selectively uptake and separate some specific substrates under ambient conditions.

To date, numerous porous MOFs with adsorption and separation properties, generally gas species (such as hydrogen, nitrogen, methane, carbon dioxide, and so on) MOF separators, have been reported.[2] In contrast, the selective adsorption and separation of aromatics,[3] especially halogenated aromatics,[4] is a relatively unexplored field. As we know, monohalobenzenes (C_6H_5X, X = F, Cl, Br, I) have been extensively used in fine chemical synthesis and in the pharmaceutical industry.[5] Since halogenated compounds are used on a wide scale, their disposal results in a large accumulation in our environment. However, they are not friendly to our environment and may cause harmful health effects. The Environment Protection Agency (EPA) and the Food and Drug Administration (FDA) found that these halogenated aromatics have some toxic effects on our ecosystem and health.[6a] For example, bromobenzene could cause liver necrosis in various animals;[6b] therefore, their enrichment and separation are very highly demanded and important.

In this contribution, we report a series of isostructural organic guest loaded Cd(II)-MOFs, namely $CdL_2(OTs)_2$·2THF (**1**), $CdL_2(OTs)_2$·$2C_6H_5F$ (**2**), $CdL_2(OTs)_2$·C_6H_5Cl (**3**), $CdL_2(OTs)_2$·$2C_6H_5Br$ (**4**), and $CdL_2(OTs)_2$·$1.5C_6H_5I$·$0.5H_2O$ (**5**), generated from 1,2-bis[(3-(pyridin-4-yl)phenoxy]-ethane and $Cd(OTs)_2$ (OTs^- = *p*-toluenesulfonate anion) in solution. After removal of the guest molecules, the guest-free $CdL_2(OTs)_2$ framework can reversibly adsorb and separate PhF, PhCl, PhBr, and PhI at room temperature in the liquid phase. Furthermore, it exhibits a guest-dependent luminescent property.

EXPERIMENTAL SECTION

Materials and Methods. All chemicals were commercially purchased and used as obtained without further purification. Infrared (IR) samples were prepared as KBr pellets, and spectra were obtained in the 400−4000 cm^{-1} range using a PerkinElmer 1600 FTIR spectrometer. Elemental analyses for C, H, and N were performed on a PerkinElmer Model 2400 analyzer. ^1H NMR data were collected using an AM-300 spectrometer. Chemical shifts are reported in δ units relative to TMS. All fluorescence measurements were carried out on a Cary Eclipse spectrofluorimeter (Varian, Belrose, Australia) equipped with a xenon lamp and quartz carrier at room temperature. Thermogravimetric analyses were performed on a TA Instrument

Received: May 12, 2014
Published: August 12, 2014

   dx.doi.org/10.1021/ic501100p | *Inorg. Chem.* 2014, 53, 9087−9094

Scheme 1. Synthesis of L and 1-5

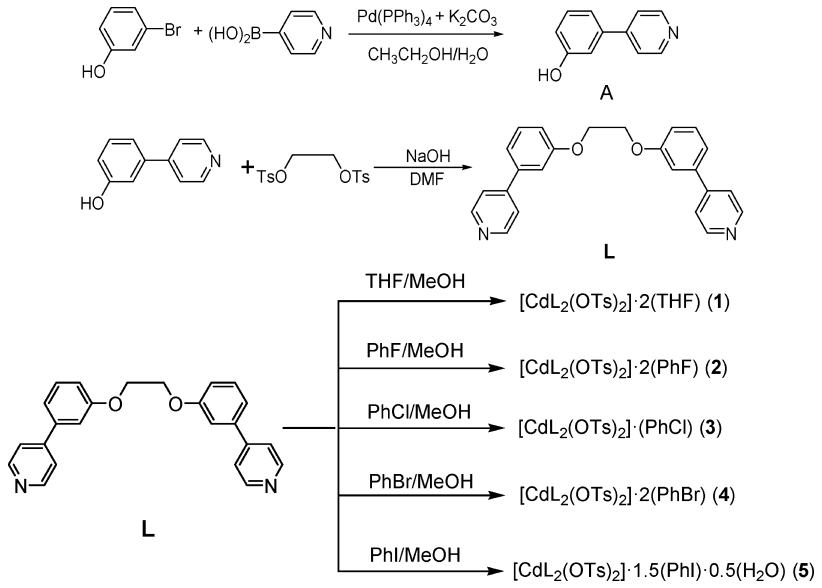

SDT 2960 simultaneous DTA-TGA under flowing nitrogen at a heating rate of 10 °C/min. Powder X-ray diffraction (PXRD) measurements were carried out on a D8 ADVANCE diffractometer with Cu Kα radiation (λ = 1.5405 Å). GC analysis was performed on a 7890A gas chromatograph (Agilent Technologies, Santa Clara, CA, USA) equipped with a flame ionization detector (FID) and a split/splitless injector. The GC capillary column (DB-WAX) with dimensions of 30 m length × 0.53 mm i.d. and a film thickness of 1.0 μm was purchased from Agilent Technologies.

Synthesis of Intermediate 3-(Pyridin-4-yl)phenol (A).[7] A solution of 3-bromophenol (3.46 g, 20.0 mmol), pyridine-4-boronic acid (2.95 g, 24.0 mmol), K_2CO_3 (17.25 g, 125.0 mmol), and $Pd(PPh_3)_4$ (1.16 g, 1.0 mmol) in EtOH/H_2O was refluxed for 40 h (Scheme 1). After removal of solvent under vacuum, the residue was purified by column chromatography to afford **A** in 82% yield. IR (KBr pellet, cm^{-1}): 3415 (m), 3053 (m), 1603 (s), 1544 (s), 1511 (w), 1476 (s), 1419 (m), 1368 (s), 1309 (s), 1210 (s), 1067 (m), 1010 (s), 897 (s), 879 (s), 833 (s), 775 (s), 725 (m), 694 (m), 665 (m), 616 (w), 538 (m). ^{1}H NMR (300 MHz, DMSO-d_6, 25 °C, TMS, ppm): 9.69 (s, 1H, −OH), 8.60−8.59 (d, 2H, $-C_6H_4-$), 7.62−7.60 (d, 2H, $-C_6H_4-$), 7.33−7.28 (t, 1H, $-C_5H_4N$), 7.20−7.17 (d, 1H, $-C_5H_4N$), 7.12 (s, 2H, $-C_5H_4N$), 6.87−6.85 (d, 2H, $-C_5H_4N$). Anal. Calcd for $C_{11}H_9NO$: C, 77.17; H, 5.30; N, 8.18. Found: C, 77.21; H, 5.42; N, 8.05.

Synthesis of L. A mixture of **A** (1.88 g, 11.0 mmol), NaOH (0.44 g, 11.0 mmol) and 1,2-bis(*p*-tolylsulfonyl)ethane (1.85 g, 5.0 mmol) was stirred in DMF (50 mL) at 358 K for 24 h and then cooled to room temperature (Scheme 1). The mixture was poured into ice−water, filtered, and washed with water. The raw product was purified by column chromatography to afford white solids in 80% yield. IR (KBr pellet, cm^{-1}): 3446 (s), 2360 (w), 1594 (s), 1580 (s), 1547 (s), 1472 (m), 1443 (w), 1409 (w), 1300 (s), 1279 (w), 1208 (s), 1175 (w), 1058 (s), 1039 (w), 994 (w), 875 (w), 819 (w), 790 (s), 727 (m), 699 (m), 615 (w), 537 (w). ^{1}H NMR (300 MHz, DMSO-d_6, 25 °C, TMS, ppm): 8.62−8.60 (d, 4H, $-C_5H_4N$), 7.72−7.71 (d, 4H, $-C_5H_4N$), 7.48−7.42 (t, 2H, $-C_6H_4-$), 7.39 (s, 4H, $-C_6H_4-$), 7.11−7.09 (d, 2H, $-C_6H_4-$), 4.40 (s, 4H, $-CH_2-$). Anal. Calcd for $C_{24}H_{20}N_2O_2$: C, 78.24; H, 5.47; N, 7.60. Found: C, 78.09; H, 5.68; N, 7.41.

Synthesis of $[CdL_2(OTs)_2]\cdot 2THF$ (1). A solution of $Cd(OTs)_2$ (27 mg, 0.060 mmol) in MeOH (8 mL) was carefully layered on a solution of **L** (15 mg, 0.040 mmol) in THF (8 mL). The solution was left for 1 week at room temperature, and colorless crystals of **1** were obtained. Yield: 72% (based on **L**). IR (KBr pellet, cm^{-1}): 3067 (w), 2931 (w), 1607 (s), 1548 (s), 1480 (m), 1418 (m), 1299 (m), 1244 (s), 1205 (s), 1161 (s), 1036 (s), 821 (m), 775 (s), 681 (s), 622 (m), 564 (s). Anal. Calcd for $C_{70}H_{70}CdN_4O_{12}S_2$: C, 62.88; H, 5.24; N, 4.19. Found: C, 62.44; H, 4.87; N, 4.01.

Synthesis of $[CdL_2(OTs)_2]\cdot 2C_6H_5F$ (2). A solution of $Cd(OTs)_2$ (10 mg, 0.022 mmol) in MeOH (2 mL) was carefully layered on a solution of **L** (5 mg, 0.013 mmol) in C_6H_5F (2 mL). The solution was left for 1 month at room temperature, and colorless crystals of **2** were obtained. Yield: 50% (based on **L**). IR (KBr pellet, cm^{-1}): 3069 (w), 2930 (w), 1607 (s), 1548 (s), 1479 (m), 1418 (m), 1299 (s), 1244 (s), 1205 (s), 1161 (s), 1036 (s), 821 (m), 776 (s), 681 (s), 622 (m), 564 (s). Anal. Calcd for $C_{74}H_{64}CdF_2N_4O_{10}S_2$: C, 64.17; H, 4.62; N, 4.05. Found: C, 63.83; H, 4.65; N, 3.84.

Synthesis of $[CdL_2(OTs)_2]\cdot C_6H_5Cl$ (3). A solution of $Cd(OTs)_2$ (27 mg, 0.060 mmol) in MeOH (8 mL) was carefully layered on a solution of **L** (15 mg, 0.040 mmol) in C_6H_5Cl (8 mL). The solution was left for 1 week at room temperature, and colorless crystals of **3** were obtained. Yield: 65% (based on **L**). IR (KBr pellet, cm^{-1}): 3067 (w), 2932 (w), 1607 (s), 1549 (s), 1477 (m), 1419 (m), 1298 (m), 1244 (s), 1206 (s), 1161 (s), 1036 (s), 821 (m), 776 (s), 680 (s), 621 (m), 564 (s). Anal. Calcd for $C_{68}H_{59}CdClN_4O_{10}S_2$: C, 62.57; H, 4.52; N, 4.29. Found: C, 62.13; H, 4.56; N, 3.95.

Synthesis of $[CdL_2(OTs)_2]\cdot 2C_6H_5Br$ (4). A solution of $Cd(OTs)_2$ (27 mg, 0.060 mmol) in MeOH (8 mL) was carefully layered on a solution of **L** (15 mg, 0.040 mmol) in C_6H_5Br (8 mL). The solution was left for 1 week at room temperature, and colorless crystals of **4** were obtained. Yield: 68% (based on **L**). IR (KBr pellet, cm^{-1}): 3068 (w), 2932 (w), 1608 (s), 1548 (s), 1476 (m), 1419 (m), 1298 (m), 1244 (s), 1205 (s), 1161 (s), 1036 (s), 822 (m), 776 (s), 680 (s), 621 (m), 564 (s). Anal. Calcd for $C_{74}H_{64}CdBr_2N_4O_{10}S_2$: C, 58.98; H, 4.25; N, 3.72. Found: C, 58.88; H, 4.35; N, 3.34.

Synthesis of $[CdL_2(OTs)_2]\cdot 1.5C_6H_5I\cdot 0.5H_2O$ (5). A solution of $Cd(OTs)_2$ (10 mg, 0.022 mmol) in MeOH (2 mL) was carefully layered on a solution of **L** (5 mg, 0.013 mmol) in C_6H_5I (2 mL). The solution was left for 1 month at room temperature, and light yellow crystals of **5** were obtained. Yield: 30% (based on **L**). IR (KBr pellet, cm^{-1}): 3069 (w), 2921 (w), 1607 (s), 1548 (s), 1479 (m), 1418 (m), 1299 (m), 1245 (s), 1206 (s), 1162 (s), 1036 (s), 821 (m), 820 (m), 776 (s), 681 (s), 622 (m), 564 (s). Anal. Calcd for $C_{71}H_{62.5}CdI_{1.5}N_4O_{10.5}S_2$: C, 56.55; H, 4.15; N, 3.72. Found: C, 56.19; H, 4.05; N, 3.75.

Compounds **1**−**5** are insoluble in common organic solvents such as acetone, THF, benzene, toluene and xylene, but they are dissociated in DMSO at room temperature.

X-ray Crystallography. The X-ray diffraction data for single crystals of **1**−**5** were measured at different temperatures (**1** at 105 K, **2**

dx.doi.org/10.1021/ic501100p | Inorg. Chem. 2014, 53, 9087−9094

Table 1. Crystal Data and Structural Refinement Parameters for 1−5

	1	2	3	4	5
formula	$C_{70}H_{70}CdN_4O_{12}S_2$	$C_{74}H_{64}CdF_2N_4O_{10}S_2$	$C_{68}H_{59}CdClN_4O_{10}S_2$	$C_{74}H_{64}CdBr_2N_4O_{10}S_2$	$C_{71}H_{62.5}CdI_{1.5}N_4O_{10.5}S_2$
fw	1335.82	1383.81	1304.16	1505.63	1506.62
λ (Å)	0.71073	0.71073	0.71073	0.71073	0.71073
cryst syst	monoclinic	monoclinic	monoclinic	monoclinic	monoclinic
space group	*C*2/*c*	*C*2/*c*	*C*2/*c*	*C*2/*c*	*C*2/*c*
T (K)	105(7)	99.96(10)	119.97(13)	119.99(11)	99.93(16)
a (Å)	28.5077(12)	28.3154(9)	28.5373(7)	28.6004(10)	28.561(2)
b (Å)	13.4136(4)	13.4934(4)	13.5012(3)	13.4741(3)	13.4161(5)
c (Å)	18.1780(7)	18.3088(5)	18.2192(4)	18.3173(8)	18.0696(8)
α (deg)	90.00	90.00	90.00	90.00	90.00
β (deg)	106.675(4)	106.868(3)	107.342(2)	107.463(4)	106.976(4)
γ (deg)	90.00	90.00	90.00	90.00	90.00
V (Å^3)	6658.8(4)	6694.3(3)	6700.5(3)	6733.5(4)	6622.2(6)
Z	4	4	4	4	4
ρ_{cakd} (g cm^{-3})	1.332	1.373	1.293	1.485	1.511
μ (mm^{-1})	0.454	0.457	0.486	1.636	1.155
F(000)	2776	2856	2688	3064	3040
GOF	1.062	1.104	1.130	1.040	1.033
no. of data/restraints/params	5867/0/448	5900/0/482	5907/0/534	5885/0/486	6149/91/479
R1 ($I > 2\sigma(I)$)	0.0551	0.0571	0.0541	0.0824	0.0601
wR2 (all data)	0.1626	0.1755	0.1769	0.2274	0.1646

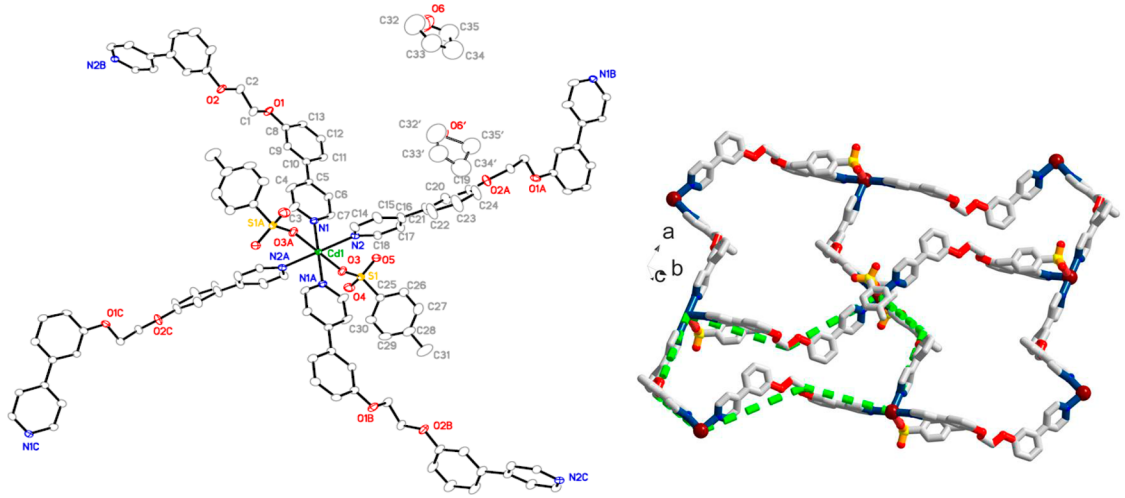

Figure 1. (a) ORTEP figure of **1**. (b) 2D network of **1** with a twist-boat-like window. The single twist-boat unit is highlighted by a dashed line in green.

and **5** at 100 K, **3** and **4** at 120 K) on an Agilent Technologies SuperNova Single Crystal Diffractometer with graphite-monochromated Mo Kα radiation (λ = 0.71073 Å). Corrections for incident and diffracted beam absorption effects were applied using CrysAlisPro.[8] None of the crystals showed evidence of crystal decay during data collection. The structures were solved by direct methods using the SHELXS program and refined by full matrix least squares on F^2, including all reflections (SHELXL97).[9] The crystal data, refinement parameters, and bond lengths and angles are summarized in Table 1 and in the Supporting Information.

RESULTS AND DISCUSSION

Synthesis and Crystal Structures. Compound **1** ($2THF{\subset}CdL_2(OTs)_2$) was obtained by the combination of **L** and $Cd(OTs)_2$ in a THF/MeOH mixed-solvent system in 72% yield, while compounds **2** ($2C_6H_5F{\subset}CdL_2(OTs)_2$), **3** ($C_6H_5Cl{\subset}CdL_2(OTs)_2$), **4** ($2C_6H_5Br{\subset}CdL_2(OTs)_2$), and **5** ($1.5C_6H_5I{\cdot}0.5H_2O{\subset}CdL_2(OTs)_2$) were prepared by the combination of **L** with $Cd(OTs)_2$ in the mixed-solvent systems consisting of MeOH and the corresponding monohalobenzene in 30−68% yields. The results demonstrated that THF and monohalobenzenes (PhF, PhCl, PhBr, and PhI) can be the templates to facilitate the formation of the porous frameworks of **1**−**5**. X-ray single-crystal analyses revealed that compounds **1**−**5** are isostructural and all crystallize in the triclinic space group *C*2/*c* (Table 1, Figures S1−S5 (Supporting Information)). The cell volumes of **1**−**5** are slightly different (variation from 6622.2(6) to 6733.5(4) Å^3, Table 1) due to the encapsulation of different guest species. Therefore, only the structure of **1** is described in detail herein.

As shown in Figure 1, the asymmetric unit cell of **1** consists of half of a Cd(II) ion, one **L** ligand, one OTs^- anion, and one THF guest molecule. Each Cd(II) node lies in a distorted-octahedral coordination environment which consists of four N atoms from four **L** ligands in the equatorial plane and two O atoms from two OTs^- anions in the axial positions. The Cd−N bond lengths vary from 2.333(3) to 2.328(3) Å, while the Cd−

dx.doi.org/10.1021/ic501100p | Inorg. Chem. 2014, 53, 9087−9094

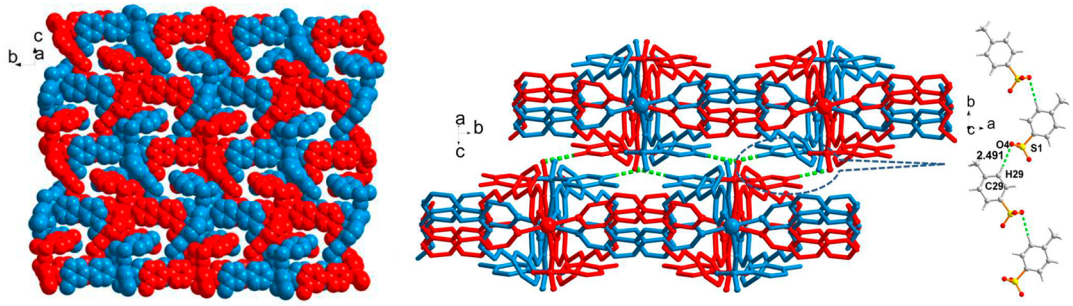

Figure 2. (left) Single 2-fold interpenetrating layers of **1**. The different sets of 2D nets are shown in different colors for clarity. (right) Interlayer hydrogen bonding systems.

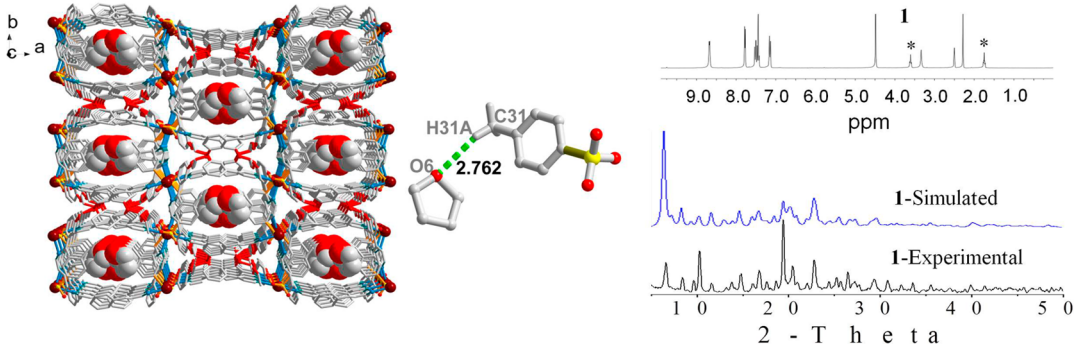

Figure 3. (left) Stacking of 2D layers in an −ABAB− fashion into a 3D framework with 1D channels along the crystallographic *c* axis, in which THF guest molecules are located. The encapsulated THF molecules are shown as space-filling models for clarity. (right) ^{1}H NMR (DMSO-d_6) spectrum and XRPD patterns of **1**. The H peaks corresponding to the encapsulated THF molecules are marked with asterisks.

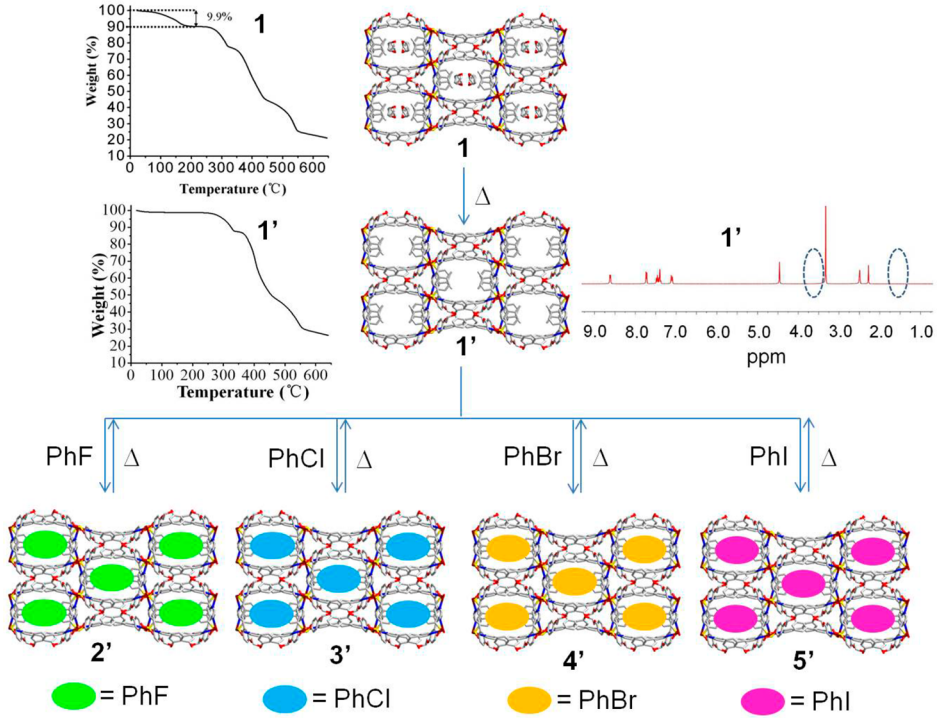

Figure 4. Synthesis of the hollow framework $CdL_2(OTs)_2$ (**1**′) and reversible adsorption of monohalobenzenes based on **1**′. The encapsulated PhF, PhCl, PhBr, and PhI are shown in green, cyan, orange, and purple, respectively. The TGA traces of **1** and **1**′ (the observed THF mass loss in **1** is 9.9%, calculated 10.8%) and ^{1}H NMR ((DMSO-d_6) of **1**′ are shown as inserts.

O bond length is 2.306(3) Å (Tables S1−S5 (Supporting Information)). In **1**, each **L** adopts a *gauche* conformation with a torsion angle (−O−CH_2−CH_2−O−) of 73.004(4)°. As a node, each Cd(II) atom connects to four adjacent Cd(II) atoms via four bidentate **L** ligands, forming a four-connected (4,4) network structure. The 2D layered net contains a twist-

dx.doi.org/10.1021/ic501100p | *Inorg. Chem.* 2014, 53, 9087−9094

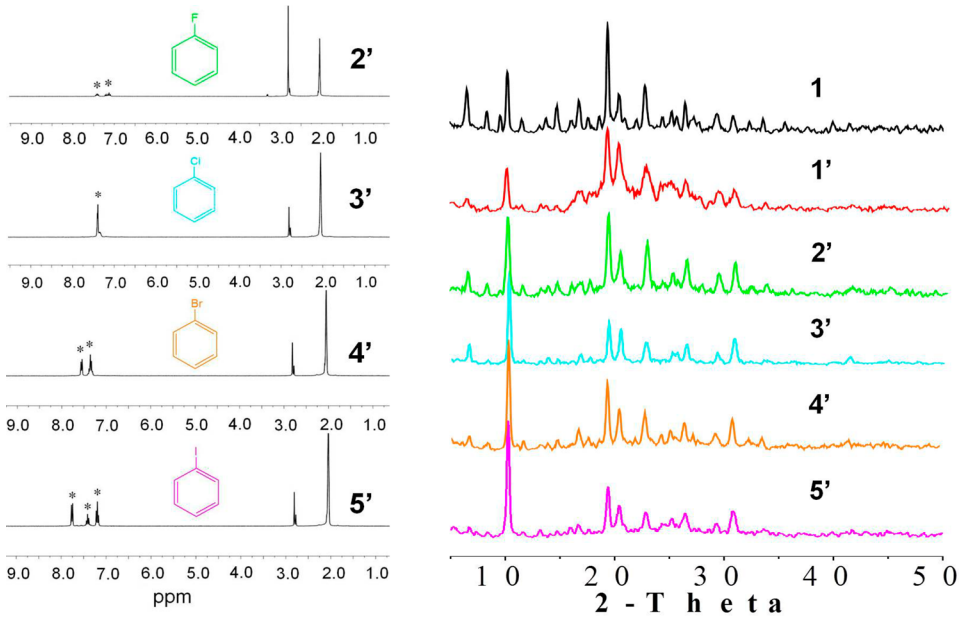

Figure 5. (left) ^{1}H NMR (CD_3COCD_3) performed on CD_3COCD_3 extracts of **2′**−**5′**. (right) XRPD patterns of **2′**−**5′**.

boat-like window with a Cd···Cd distance of 19.7828(6) Å (Figure 1).

Furthermore, two equivalent sets of such 2D nets interweave with each other to generate a 2-fold interpenetrating layer extended in the crystallographic *bc* plane. As shown in Figure 2, the Cd(II) nodes in one set of 2D nets occupy the center of the void formed by the other. On further inspection, we found that there are weak hydrogen bonding systems[10] (O(4)···H(29) = 2.491 Å, O(4)···H(29) = 3.419 Å and ∠C(29)−H(29)−O(4) = 175°) consisting of the coordinated OTs^- anions located in the adjacent interpenetrating 2D layers, which make these layers stack in an −ABAB− fashion (Figure 2) to form a 3D porous supermolecular structure (Figure 3). Meanwhile, 1D squarelike channels were formed with the dimensions of ∼7.7 × 8.8 Å^2 along the *c* axis, in which THF solvent molecules are located (Figure 3). The THF guest molecules are fixed inside through weak intermolecular hydrogen-bonding interactions[10] composed of the coordinated OTs^- anion and the uploaded THF molecule (Figure 3). The ^{1}H NMR (DMSO-d_6) spectrum of **1** further confirmed the existence of THF in **1** (Figure 3). The XRPD pattern of **1** indicates that the compound was obtained in a pure phase (Figure 3).

Similarly to **1**, all of the monohalobenzene guests in **2**−**5** are located in the ellipselike channels and are weakly hydrogen bonded to the framework through interhost−guest X···H−C (X = F, Cl, Br, I) bonds.[10] The weak hydrogen-bonding systems consist of the halogen atoms, OTs^- anion, and **L** ligand. The X···H (X = F, Cl, Br, I) distances are in the range 2.766−3.293 Å. Different from the case for **2**−**4**, 0.5 water molecule per formula unit exists in the pores of **5** in addition to PhI. The different encapsulated monohalobenzenes are further confirmed by the corresponding ^{1}H NMR spectra (Figure S6 (Supporting Information)). The corresponding PXRD patterns demonstrated that compounds **2**−**5** are obtained in pure phases (Figure S6).

Notably, X-ray single-crystal analysis indicated that the numbers of encapsulated monohalobenzenes in **2**−**5** are different. For example, there are two PhX guest molecules per formula in **2** ($2C_6H_5F{\subset}CdL_2$) and **4** ($2C_6H_5Br{\subset}CdL_2$), while only one PhX per formula is found in **3** ($C_6H_5Cl{\subset}CdL_2$) and 1.5 PhX guest molecules are found in **5** ($1.5C_6H_5I{\subset}CdL_2$). Although it is not clear from this study why CdL_2 contains different numbers of lattice PhX molecules for the different monohalobenzenes, the thermogravimeric analysis (TGA) is in good agreement with the X-ray single-crystal analysis (Figure S7 (Supporting Information)).

Reversible Adsorption. Our experiment demonstrated that **1** is able to reversibly uptake monohalobenzene species in the liquid phase. The guest-free host framework of **1** was obtained by heating of the crystals at 150 °C for 2 h (monitored by TGA measurements). The ^{1}H NMR (DMSO-d_6) spectrum of the desolvated sample **1′** clearly indicated that the uploaded THF molecules were completely removed (Figure 4). The XPRD patterns of the corresponding solid **1′** displayed that the shapes and intensities of reflections are almost identical with those of **1**, meaning that guest loss did not result in symmetry change or cavity volume collapse (Figure 5).

In addition, when **1′** was respectively immersed in PhF, PhCl, PhBr, and PhI for 10 h (no difference in adsorption amount was observed at longer times) at ambient temperature, the monohalobenzenes were taken inside to generate $PhX{\subset}CdL_2(OTs)_2$ (X = F (**2′**), Cl (**3′**), Br (**4′**), I (**5′**)). As shown in Figure 5, the ^{1}H NMR spectra of **2′**−**5′** of their acetone-d_6 extracts indicated that the monohalobenzenes are present in the channels, and the adsorption amounts of PhF, PhCl, PhBr, and PhI are up to 6.3, 7.5, 11.9, and 5.8%, respectively, on the basis of TGA measurements (Figure S8 (Supporting Information)). The PXRD patterns of **2′**−**5′** indicated that the framework of **1** was retained in the processes of the monohalobenzene adsorption (Figure 5). The halobenzene-free framework of **1′** can be regenerated by heating (150 °C for 2 h) of the $PhX{\subset}CdL_2(OTs)_2$ compounds (Figure S9 (Supporting Information)). On the other hand, the encapsulated halobenzene guests can also be completely removed by solid−liquid extraction (Figure S10 (Supporting Information)). Therefore, the PhX adsorption based on the CdL_2 framework is reversible. Additionally, the THF guest molecules of **1** could be directly exchanged by the

dx.doi.org/10.1021/ic501100p | *Inorg. Chem.* 2014, 53, 9087−9094

monohalobenzenes to generate the corresponding $PhX\subset CdL_2(OTs)_2$ when **1** was immersed in the monohalobenzene solvents at ambient temperature (Figure S11 (Supporting Information)).

Monohalobenzene Separation. As we know, the major hurdle in molecular separation is guest selectivity for capturing a specific substrate in the presence of one or several different potential competitors. In principle, suitable MOFs constructed by the rational combination of subtly designed organic ligands and metal ions are able to selectively absorb one type of monohalobenzene in the presence of other kinds of homologues. Additionally, separation via adsorption based on MOF adsorbents might be a more energy efficient approach than that of distillation; thus, the development of new types of MOF adsorbents is very significant. To explore the possibility of separating these monohalobenzenes in the liquid phase, the experiments were designed to test the binding affinity of the CdL_2 host framework for PhF, PhCl, PhBr, or PhI in the presence of other monohalobenzenes (Figure 6). After the

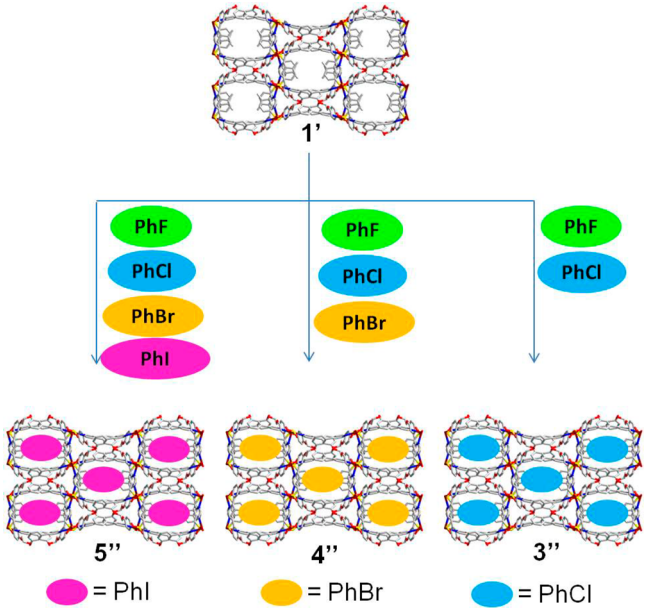

Figure 6. Separation of monohalobenzenes based on the CdL_2 framework. The PhX species are shown as ellipses in different colors for clarity. The crystallographic lengths for PhX are ca. 4.1 (PhF), 4.3 (PhCl), 4.6 (PhBr), and 4.9 Å (PhI).

desolvated sample of **1′** was immersed in a mixed-solvent system consisting of equimolar amounts of PhF/PhCl/PhBr/PhI at ambient temperature for 10 h, the resulting crystalline powder was extracted with acetone-d_6. The ^{1}H NMR spectrum of the acetone-d_6 extract showed that three sets of chemical shifts are located between 7 and 8 ppm, indicating the presence of pure PhI (Figure S12a (Supporting Information)). Therefore, CdL_2 is able to separate PhI from a PhF/PhCl/PhBr mixture to give rise to $PhI\subset CdL_2(OTs)_2$ (**5″**). Similarly, when the desolvated sample of **1′** was soaked in a mixture of equimolar amounts of PhF/PhCl/PhBr under the same conditions, the two sets of signals at 7.25−7.75 ppm in the ^{1}H NMR spectrum (Figure S12b) of the acetone-d_6 extract clearly evidenced that only PhBr was uploaded to form $PhBr\subset CdL_2(OTs)_2$ (**4″**). In addition to separation of PhI and PhBr, CdL_2 is still able to completely separate PhCl from PhF in the liquid phase at ambient temperature. When the crystals of **1′** were suspended in a PhCl/PhF mixed solvent (molar ratio 1:1) at room temperature for 10 h, the ^{1}H NMR spectrum of the acetone-d_6 extract showed that only PhCl was taken up by the framework to result in the formation of $PhCl\subset CdL_2(OTs)_2$ (**3″**, Figure S12c). Again, the corresponding XRPD patterns indicated that the CdL_2 framework is intact during the selective process (Figure S12). Notably, the monohalobenzene occluded $CdL_2(OTs)_2$ could be directly exchanged by the reverse affinity sequence of monohalobenzene. For example, when $PhI\subset CdL_2(OTs)_2$ was soaked in PhBr (large excess) for 10 h, the loaded PhI molecules were replaced by PhBr, which was demonstrated by ^{1}H NMR spectrum (Figure S13 (Supporting Information)).

In order to further evidence the results, the above acetone extracts were used to perform the gas chromatographic analysis (Supporting Information). The results of GC analysis are in good agreement with the above discussion. The standard sample was prepared by mixing equimolar amounts of PhF, PhCl, PhBr, and PhI in acetone (Figure 7a). As shown in

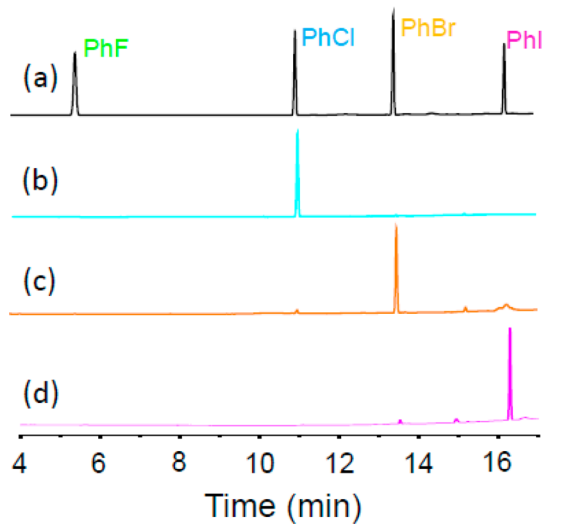

Figure 7. GC analysis: (a) standard sample composed of PhX (X = F, Cl, Br, I) in acetone; (b) acetone extract of **1′** immersed in a mixed solvent of equimolar amounts of PhF/PhCl; (c) acetone extract of **1′** immersed in the mixed solvent of equimolar amounts of PhF/PhCl/PhBr; (d) acetone extract of **1′** immersed in the mixed solvent of equimolar amounts of PhF/PhCl/PhBr/PhI.

Figure 7b, no PhF species was detected by GC analysis in the acetone extract which was obtained by immersing **1′** in a mixed solvent of equimolar amounts of PhF/PhCl, indicating that the PhCl is pure. Chromatographic measurement (Figure 7c) on the acetone extract of **1′** immersed in a PhF/PhCl/PhBr mixture (molar ratio 1/1/1) indicated that no PhF species was found, but a tiny amount of PhCl coexisted there, and the purity of PhBr was 96.3%. Figure 7d shows that a tiny amount of PhBr coexisted with PhI when **1′** was used to separate PhI from a mixture composed of equimolar amounts of PhF/PhCl/PhBr/PhI. GC analysis confirmed that the purity of the PhI is 96.1%. In comparison to GC analysis, the corresponding PhX impurities could not be clearly detected by the ^{1}H NMR spectrum due to its higher detection limit.

On the basis of the above discussion, the CdL_2 framework exhibits a clear affinity for the monohalobenzenes and obeys the sequence PhI > PhBr > PhCl > PhF. Obviously, guest

dx.doi.org/10.1021/ic501100p | Inorg. Chem. 2014, 53, 9087−9094

dimension and shape are not the dominating factors for the selectivity, which is quite different from what was found in our previous studies.[11] Single-crystal analysis revealed that the squarelike channels in **1** are surrounded by the methyl groups and aromatic rings to provide a nonpolar microenvironment, so that the less polar guest species (dielectric constant ε_r = 5.465 (PhF), 5.6895 (PhBr), 5.45 (PhBr), 4.59 (PhI)) might be preferentially taken up by the host framework.[12] Therefore, the affinity herein could be driven by the guest polarity instead of size and shape.

Guest-Dependent Luminescent Properties. In addition, these monohalobenzene⊂CdL_2 host–guest systems show an interesting guest-dependent photoluminescence. As shown in Figure 8, the guest-free CdL_2 framework **1′** and monohalobenzene⊂CdL_2 host–guest systems **2**–**5** all exhibit blue-purple emissions at λ_{ex} = 419–425 nm upon excitation at λ_{em} 323 nm, but with different intensities. Figure 8 shows that the emission intensity decreases on going from **2** to **5**, which is in good agreement with what is expected on the basis of the heavy-atom effect.[13] In comparison to **2**–**4**, the emission of **1′** is less intense. This could be attributed to the encapsulated PhX molecules that enhance the rigidity of the CdL_2 host framework and consequently the intraligand π–π^* energy.[11a] Such guest-dependent luminescence properties[14] demonstrate that the Cd(II)-MOF herein might have potential application as a sensor for detecting monohalobenzene species.

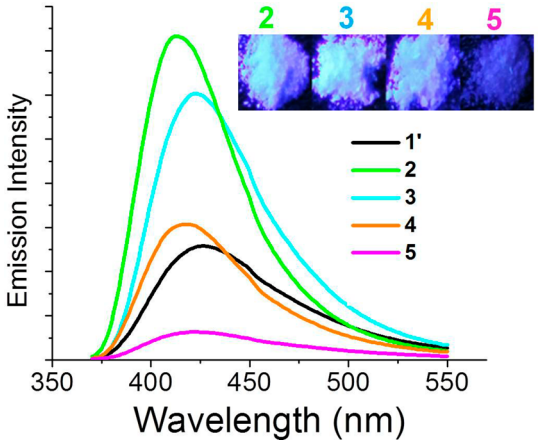

Figure 8. Photoinduced solid-state emission spectra of **1′** and **2**–**5**. Samples of **2**–**5** illuminated with UV light are shown as inserts.

CONCLUSIONS

In summary, five host–guest metal-organic frameworks Guest⊂$CdL_2(OTs)_2$ have been synthesized from the flexible open-chain polyether-bridged ligand **L** and $Cd(OTs)_2$. The guest-free host framework $CdL_2(OTs)_2$ **1′** is reusable and can reversibly adsorb monohalobenzenes C_6H_5X (X = F, Cl, Br, I); furthermore, it can effectively separate these monohalobenzenes in the liquid phase under ambient conditions. In addition, the luminescence intensities of the PhX-loaded Cd(II)-MOF are different and exhibit guest-dependent luminescence properties.

ASSOCIATED CONTENT

Supporting Information

Figures, tables, and CIF files giving crystallographic data fpr **1**–**5** and GC analysis. This material is available free of charge via the Internet at http://pubs.acs.org.

AUTHOR INFORMATION

Corresponding Author

*E-mail for Y.-B.D.: yubindong@sdnu.edu.cn.

Notes

The authors declare no competing financial interest.

ACKNOWLEDGMENTS

We are grateful for financial support from the 973 Program (Grant Nos. 2012CB821705 and 2013CB933800), the NSFC (Grant Nos. 21271120), the Taishan scholar's construction project special fund, and "PCSIRT".

REFERENCES

(1) (a) Deng, H.; Grunder, S.; Cordova, K. E.; Valente, C.; Furukawa, H.; Hmadeh, M.; Gándara, F.; Whalley, A. C.; Liu, Z.; Asahina, S.; Kazumori, H.; O'Keeffe, M.; Terasaki, O.; Stoddart, J. F.; Yaghi, O. M. *Science* **2012**, *336*, 1018–1023. (b) Li, J.-R.; Sculley, J.; Zhou, H.-C. *Chem. Rev.* **2012**, *112*, 869–932. (c) Wu, H.; Gong, Q.; Olson, D. H.; Li, J. *Chem. Rev.* **2012**, *112*, 836–868. (d) Kreno, L. E.; Leong, K.; Farha, O. K.; Allendorf, M.; Van Duyne, R. P.; Hupp, J. T. *Chem. Rev.* **2012**, *112*, 1105–1125. (e) Sumida, K.; Rogow, D. L.; Mason, J. A.; McDonald, T. M.; Bloch, E. D.; Herm, Z. R.; Bae, T.-H.; Long, J. R. *Chem. Rev.* **2012**, *112*, 724–781.

(2) (a) Eddaoudi, M.; Kim, J.; Rosi, N.; Vodak, D.; Wachter, J.; O'Keeffe, M.; Yaghi, O. *Science* **2002**, *295*, 469–472. (b) Phan, A.; Doonan, C. J.; Uribe-Romo, F. J.; Knobler, C. B.; O'Keeffe, M.; Yaghi, O. M. *Acc. Chem. Res.* **2010**, *43*, 58–67. (c) Bourrelly, S.; Llewellyn, P.; Serre, C.; Millange, F.; Loiseau, T.; Férey, G. *J. Am. Chem. Soc.* **2005**, *127*, 13519–13521. (d) Panella, B.; Hirscher, M.; Puetter, H.; Mueller, U. *Adv. Funct. Mater.* **2006**, *16*, 520–524. (e) Liu, Y.; Eubank, J. F.; Cairns, A. J.; Eckert, J.; Kravtsov, V. C.; Luebke, R.; Eddaoudi, M. *Angew. Chem., Int. Ed.* **2007**, *46*, 3278–3283. (f) Xue, D.-X.; Cairns, A. J.; Belmabkhout, Y.; Wojtas, L.; Liu, Y.; Alkordi, M. H.; Eddaoudi, M. *J. Am. Chem. Soc.* **2013**, *135*, 7660–7667. (g) Haldoupis, E.; Nair, S.; Sholl, D. S. *J. Am. Chem. Soc.* **2012**, *134*, 4313–4323. (h) Deria, P.; Mondloch, J. E.; Tylianakis, E.; Ghosh, P.; Bury, W.; Snurr, R. Q.; Hupp, J. T.; Farha, O. K. *J. Am. Chem. Soc.* **2013**, *135*, 16801–16804. (i) Du, L.; Lu, Z.; Zheng, K.; Wang, J.; Zheng, X.; Pan, Y.; You, X.; Bai, J. *J. Am. Chem. Soc.* **2013**, *135*, 562–565. (j) Hudson, M. R.; Queen, W. L.; Mason, J. A.; Fickel, D. W.; Lobo, R. F.; Brown, C. M. *J. Am. Chem. Soc.* **2012**, *134*, 1970–1973. (k) Park, J.; Yuan, D.; Pham, K. T.; Li, J.-R.; Yakovenko, A.; Zhou, H.-C. *J. Am. Chem. Soc.* **2012**, *134*, 99–102.

(3) (a) Wang, X.; Liu, L.; Jacobson, A. J. *Angew. Chem., Int. Ed.* **2006**, *45*, 6499–6503. (b) Alaerts, L.; Maes, M.; Giebeler, L.; Jacobs, P. A.; Martens, J. A.; Denayer, J. F. M.; Kirschhock, C. E. A.; De Vos, D. E. *J. Am. Chem. Soc.* **2008**, *130*, 14170–14178. (c) Cychosz, K. A.; Wong-Foy, A. G.; Matzger, A. J. *J. Am. Chem. Soc.* **2008**, *130*, 6938–6939. (d) Alaerts, L.; Kirschhock, C. E. A.; Maes, M.; van der Veen, M. A.; Finsy, V.; Depla, A.; Martens, J. A.; Baron, G. V.; Jacobs, P. A.; Denayer, J. F. M.; De Vos, D. E. *Angew. Chem., Int. Ed.* **2007**, *46*, 4293–4297. (e) Finsy, V.; Verelst, H.; Alaerts, L.; De Vos, D.; Jacobs, P. A.; Baron, G. V.; Denayer, J. F. M. *J. Am. Chem. Soc.* **2008**, *130*, 7110–7118. (f) Maes, M.; Vermoortele, F.; Alaerts, L.; Couck, S.; Kirschhock, C. E. A.; Denayer, J. F. M.; De Vos, D. E. *J. Am. Chem. Soc.* **2010**, *132*, 15277–15285.

(4) Xu, G.; Zhang, X.; Guo, P.; Pan, C.; Zhang, H.; Wang, C. *J. Am. Chem. Soc.* **2010**, *132*, 3656–3657.

(5) Huang, H.; Wang, X.; Ou, W.; Zhao, J.; Shao, Y.; Wang, L. *Chemosphere* **2003**, *53*, 963–970.

(6) (a) Patra, A. K.; Dutta, A.; Bhaumik, A. *ACS Appl. Mater. Interfaces* **2012**, *4*, 5022−5028. (b) Reid, W. D.; Krishna, G.; Gillette, J. R.; Brodie, B. B. *Pharmacology* **1973**, *10*, 193−214.
(7) Wu, D.; Qin, N.; Liu, Q.-K.; Ma, J.-P.; Dong, Y.-B. *Acta Crystallogr., Sect. C* **2012**, *C68*, m156−160.
(8) *CrysAlisPro, Version 1.171.36.32 (release 02-08-2013 CrysAlis171.-NET)*; Agilent Technologies, Santa Clara, CA, 2013. Empirical absorption correction using spherical harmonics, implemented in the SCALE3 ABSPACK scaling algorithm.
(9) Sheldrick, G. M. *Acta Crystallogr., Sect. A* **2008**, *A64*, 112−122.
(10) (a) Desiraju, G. R. *Acc. Chem. Res.* **1996**, *29*, 441−449. (b) Lu, Y.; Wang, Y.; Xu, Z.; Yan, X.; Luo, X.; Jiang, H.; Zhu, W. *J. Phys. Chem. B* **2009**, *113*, 12615−12621.
(11) (a) Liu, Q.-K.; Ma, J.-P.; Dong, Y.-B. *Chem. Eur. J.* **2009**, *15*, 10364−10368. (b) Liu, Q.-K.; Ma, J.-P.; Dong, Y.-B. *J. Am. Chem. Soc.* **2010**, *132*, 7005−7017. (c) Duan, L.; Wu, Z.-H.; Ma, J.-P.; Wu, X.-W.; Dong, Y.-B. *Inorg. Chem.* **2010**, *49*, 11164−11173. (d) Liu, Q.-K.; Ma, J.-P.; Dong, Y.-B. *Chem. Commun.* **2011**, *47*, 12343−12345. (e) Xiao, J.; Chen, C.-X.; Liu, Q.-K.; Ma, J.-P.; Dong, Y.-B. *Cryst. Growth Des.* **2011**, *11*, 5696−5701.
(12) *CRC Handbook of Chemistry and Physics*, 90th ed.; Lide, D. R., Ed.; CRC Press/Taylor and Francis: Boca Raton, FL, 2009; CD-Rom Version 2010, pp 1062−1648.
(13) (a) Koziar, J. C.; Cowan, D. O. *Acc. Chem. Res.* **1978**, *11*, 334−341. (b) Tong, G. S. M.; Chow, P. K.; Che, C.-M. *Angew. Chem., Int. Ed.* **2010**, *49*, 9206−9209.
(14) Dong, M.-J.; Zhao, M.; Ou, S.; Zou, C.; Wu, C.-D. *Angew. Chem., Int. Ed.* **2014**, *53*, 1575−1579.